Non-peer reviewed preprint submitted to EarthArXiv

Title	*SCI-VIS: Lightweight Visibility Tagging for Coastal Camera Monitoring*
Authors	Michael Reinwald[1], Ketron Mitchell-Wynne[1], Zane D'Amico[1], Mercedes Stringer[1], Benjamin Freeston[1]
Affiliation	[1]Surfline Coastal Intelligence, Surfline/Wavetrak, Inc., San Francisco, California, U.S.A.
Corresponding author	Michael Reinwald <mreinwald@surfline.com>
ORCID	`https://orcid.org/0000-0001-8481-8392`
License	Creative Commons Attribution–NonCommercial 4.0 International (CC BY-NC 4.0)
Peer-review status	Under review at the *Journal of Coastal Research* (Technical Communication), submitted 7 September 2026
Keywords	fog detection; sea fog; glare; image degradation; deep learning; transfer; surf zone

SCI-VIS: Lightweight Visibility Tagging for Coastal Camera Monitoring

Michael Reinwald*[1], Ketron Mitchell-Wynne[1], Zane D'Amico[1], Mercedes Stringer[1], and Benjamin Freeston[1]

[1]Surfline Coastal Intelligence, Surfline/Wavetrak, Inc., San Francisco, California, U.S.A.

Abstract

Observations and measurements made from coastal cameras are conditional on the frame being interpretable. Sea fog, glare, rain and condensation on the housing, haze and low light each degrade the imagery, and the shoreline positions, wave measurements and counts derived from a degraded frame are corrupted or spurious. This paper evaluates a per-frame visibility classifier, based on a compact convolutional network, that assigns each frame one or more of six conditions (Clear, Glare, Fog, Rain/Blur, Hazy, Dark). It is trained and evaluated on 33,569 manually labelled frames from 757 cameras, labelled under a written protocol. On a 20% test split from cameras in training, primary-label accuracy is 93.1% and exact multi-rank accuracy 84.1%, against 67.9% for the majority class; per-class F1 ranges from 0.96 for Clear to 0.79 for Hazy. Under a camera-disjoint cross-validation, in which every camera is scored by a classifier that has not seen it, primary-label accuracy is 81.0%, and Fog, Hazy and Dark are recognised in fewer than half of their frames. Withholding one condition at a time from half of the cameras that have it shows the contribution of a camera's own labelled examples: recall of the withheld condition is 77% for Rain/Blur, 64% for Fog, 45% for Glare, 19% for Dark and 16% for Hazy, against 86 to 99% for the full classifier on the same frames. Reliable recognition of a camera's hazy and dark segments therefore requires labelled examples of those conditions from that camera, which sets what a network has to label and retrain on as it grows.

Additional index words: fog detection, sea fog, glare, image degradation, deep learning, transfer, surf zone.

1 Introduction

Fixed cameras are an established instrument of coastal monitoring. The Argus stations of Holman and Stanley (2007) made time-exposure imagery a source of shoreline position, sandbar morphology and runup; crowdsourced smartphone imagery extends shoreline mapping to sites without a permanent installation (Harley *et al.*, 2019); and four decades of monitoring at one Australian beach show camera records complementing survey and satellite data (Splinter, Harley, and Turner, 2018). In each of these systems the geophysical quantity is recovered from the radiometric content of a frame, so every retrieval is conditional on the atmosphere and the optics between the camera and the surf zone. Sea fog removes the horizon and the distant surf, glare saturates the water surface, rain and condensation on the housing degrade every pixel, haze lowers contrast, and low light raises sensor noise. Where a station acquires a few images a day, the affected frames are set aside by inspection. Commercial surf-camera networks record continuously at hundreds of sites, and breaking wave height, shoreline position and recreational use are extracted from that video automatically, the last of these by an object detector applied to every archived segment (Reinwald *et al.*, 2026). At that volume the frames that carry no usable signal, and those that produce false detections in the modules consuming them, have to be identified without an operator.

Visibility is spatially heterogeneous. Coastal fog is patchy and often obscures one camera while a neighbour kilometres away stays clear (Rauschenbach *et al.*, 2026), so the nearest weather station does not describe the conditions in a given camera's field of view. The assessment has to be made per camera from the imagery itself, at the cadence of the imagery.

The classifier described here, SCI-VIS, is the visibility stage of Surfline's Coastal Intelligence pipeline. The classifier reads one frame per video segment (roughly 10 minutes long each) and assigns it one or more of six conditions (Clear, Glare, Fog, Rain/Blur, Hazy, Dark), ordered by the share of the surf zone each affects, and its label determines whether that segment's downstream outputs are deemed reliable for different applications. It is a compact convolutional network trained on 33,569 manually labelled frames from 757 cameras of the network. Cameras join the network continuously; frames from a new camera are labelled when its output is judged unreliable, and the classifier is retrained, so in operation it scores cameras it has seen, though not necessarily in every condition.

This paper addresses three questions about the classifier. First, how accurately it tags the six co-occurring conditions on frames from the network, measured on a held-out test split. Second, how accurately it tags a camera it has never seen, measured by a camera-disjoint cross-validation. Third, which conditions a new camera needs a labelled example of before the classifier recognises them there, measured by withholding one condition at a time from a set of cameras. The three answers give the accuracy of the classifier in the regime it operates in and what a growing network has to label to keep it there.

1.1 Related Work

The prior work bearing on the classifier concerns coastal imaging and its quality control, image-based visibility classification, and the methods the evaluation rests on.

1.1.1 Coastal Imaging and Image Quality Control

Fixed-camera coastal monitoring dates from the Argus programme (Holman and Stanley, 2007), whose stations produce time-exposure and variance images from which shoreline position, sandbar location and runup are extracted. It now includes crowd-sourced smartphone imagery (Harley *et al.*, 2019) and multi-decade records that combine cameras, surveys and satellites (Splinter, Harley, and Turner, 2018). In these systems acquisition is scheduled by time of day, and images degraded by fog, rain or glare are identified by inspection or by the failure of a downstream product rather than by an automated per-frame classifier.

1.1.2 Image-Based Visibility and Weather Classification

Visibility distance under fog has been estimated from gradient statistics of road-scene images (Hautière *et al.*, 2006), and handcrafted contrast and edge features underlie later fog detectors (Bronte, Bergasa, and Alcantarilla, 2009). Convolutional networks have since been applied to weather and degradation classification. Lu *et al.* (2014) combined a CNN with weather-specific cues for two-class outdoor weather classification. Yang *et al.* (2023) proposed a multitask CNN cascade that classifies fog level and estimates fog visibility distance on expressway surveillance imagery. Compact ImageNet-pretrained classification networks, such as the classification variants of the YOLO family (Ultralytics, 2025), bring the inference cost of this approach to a few milliseconds per frame.

Bae *et al.* (2019) estimated visibility distance from coastal CCTV imagery using a dark-channel-prior transmission map combined with a distance-map calibration, evaluated at three Korean ports. Sea fog is common in coastal regions due to advection of warm moist air over cold ocean surfaces (Lewis *et al.*, 2003), and its optical properties differ from continental fog. Rauschenbach *et al.* (2026) applied image-based fog detection to the same class of imagery: five of their six Oregon-coast camera sites are Surfline cameras drawn from the network studied here. They compute the nine Fog-Aware Statistical Features of Choi, You, and Bovik (2015), which descend from the natural-scene-statistics approach to no-reference image quality assessment (Mittal, Moorthy, and Bovik, 2012), over three horizontal image strips and classify fog presence with a Gaussian-process classifier, reaching a fog F1 of 0.87. Their formulation is binary (fog / no fog), tied to World Meteorological Organization visibility thresholds, and validated against a forward-scatter visibility sensor at a nearby airport; it is complementary to the multi-condition, network-scale tagging task addressed here.

1.1.3 Multi-Label Encoding and Grouped Evaluation

Assigning several labels to one image is multi-label classification (Boutell *et al.*, 2004; Tsoumakas and Katakis, 2007). Treating each observed combination of labels as one class of a single multi-class problem is the label-powerset transformation, and requiring the whole predicted label set to equal the true one is subset accuracy. When observations are grouped, by site, time or camera, a random cross-validation partition places members of one group on both sides of the split and estimates accuracy within the sampled groups, whereas a partition blocked by group estimates transfer to unseen groups (Roberts *et al.*, 2017).

2 Methods

The classifier maps a frame to an ordered string of up to three visibility conditions and is trained and evaluated on manually labelled still frames from the camera network. The labelled corpus, the label scheme and the encoding of the ordered labels are described first, then the network and its training, then the three evaluation protocols. Each protocol scores a different regime: frames from cameras in training, cameras absent from training, and cameras in training that carry no example of the condition being scored.

2.1 Data

Labelled frames come from the camera network, and their visibility conditions are judged over the surf zone by annotators following a written guide.

2.1.1 Dataset Overview

The dataset consists of 33,569 still frames from 757 cameras of the network, at sites in the continental United States, Hawaii, Central America, Indonesia, Australia and Europe, captured between 2020 and 2023. Frame height is 720 pixels for 77.7% of them and 1,080 pixels for 7.6%; the remaining 14.7% come from lower-resolution feeds and are 270 to 576 pixels high.

Frames are unevenly distributed over cameras: the median camera contributes 13 frames, and 241 cameras with more than 20 frames each supply 27,775 frames (83% of the dataset), a concentration examined in the Cameras Absent From Training subsection. Figure 1 summarises the per-condition frame counts; the "primary-label" class is the condition the annotator judged to occupy the largest share of the surf zone in each frame. Clear is the primary label of 68% of the frames, and 12,586 frames (37%) carry a second or third condition.

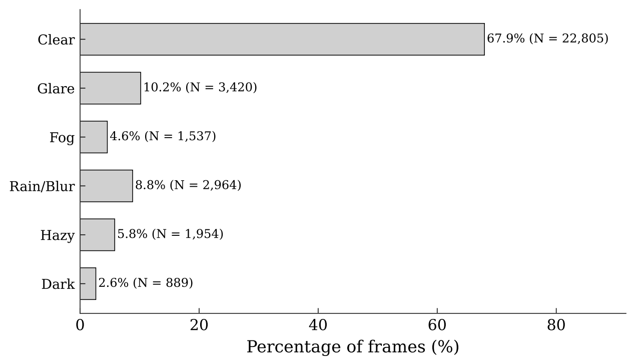

Figure 1: Distribution of primary-label visibility conditions over the 33,569 labelled frames. Each bar gives the fraction of frames whose primary label is the condition named on the left, annotated with the frame count. The figure establishes the class imbalance that shapes the error structure reported in the Results section: Clear holds 68% of the frames, Hazy 5.8% and Dark 2.6%.

2.1.2 Class Taxonomy

The six visibility conditions are defined as follows:

- Clear (0): Good visibility, no atmospheric or optical artefacts. The horizon and surf zone are clearly resolved.
- Glare (1): Sun glare on the sensor or water surface, causing partial or full saturation and loss of contrast in the affected region.
- Fog (2): Low-lying or advection fog obscuring the horizon and distant surf, reducing contrast and blurring distant features.
- Rain/Blur (3): Rain droplets on the lens, optical blur, or precipitation visible in the scene, reducing image sharpness.
- Hazy (4): Atmospheric haze or sea spray reducing contrast without complete obscuration. Distinguished from Fog by the presence of a discernible but degraded horizon.
- Dark (5): Low-light conditions (pre-dawn, post-dusk, overcast night) that result in reduced dynamic range and elevated sensor noise.

Figure 2 shows representative frames for each condition.

2.1.3 Annotation Methodology

Frames are labelled by a small team of trained annotators following an internal written labelling guide. The guide fixes the definition of each of the six conditions and carries reference frames for each single condition and for the transitional two- and three-rank combinations; those reference frames are reproduced in Figure 3. No inter-annotator agreement study was conducted (the Limitations subsection).

The schema is multi-rank: each frame carries up to three ordered labels, drawn from the six conditions. When two or more conditions co-occur in distinct parts in the field-of-view, annotators rank them by the fraction of surf-zone area each condition affects: the condition occupying the largest share is the primary label, the next largest the secondary, and so on. A frame whose surf zone is roughly 70% clear water with glare covering the remaining 30%, for example, is labelled Primary = Clear, Secondary = Glare; a single-condition frame uses only the primary slot. The reversed two-rank pairs in Figure 3 (Clear, Glare against Glare, Clear, for example) show the convention: the same pair of conditions receives opposite rank orderings depending on which condition affects more of the surf zone.

2.1.4 Label Encoding

Each frame's ordered labels are concatenated into a string, and each of the 91 combinations observed in the corpus is treated as one class of a single multi-class problem: a frame labelled Clear, Glare maps to "01" and a frame labelled Fog alone to "2". This label-powerset transformation preserves rank order and cannot predict a combination absent from training.

Exact multi-rank accuracy, subset accuracy in multi-label terms, requires the predicted string to equal the ground-truth string. Primary-label accuracy compares only the first condition of each string and reduces the comparison to a six-class problem. Per-class precision, recall and F1 and the confusion matrix are computed on primary labels, and macro-F1 is the unweighted mean of the six per-class F1 values, which gives each condition equal weight irrespective of how many frames carry it.

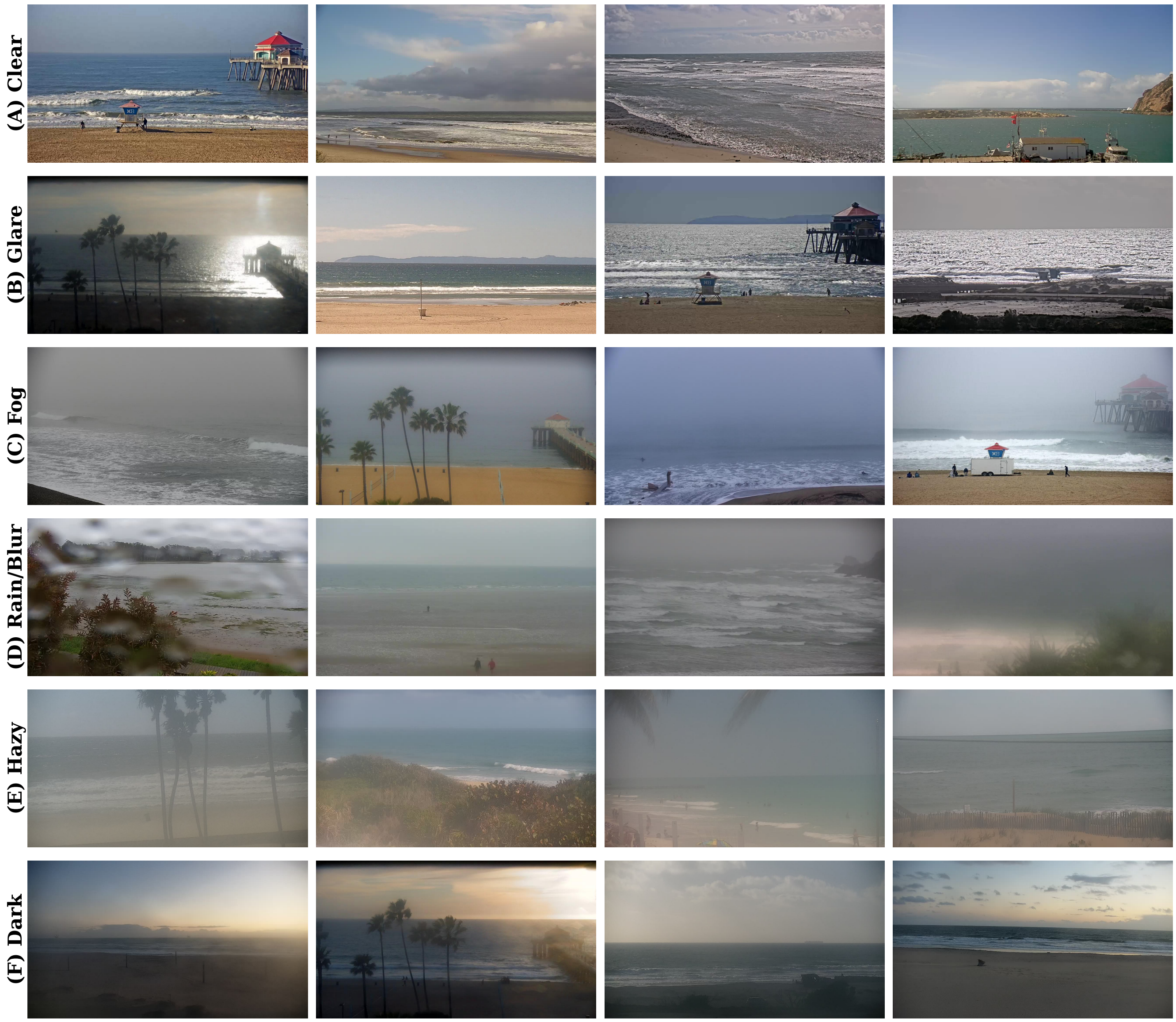

Figure 2: Representative frames for each of the six visibility conditions, four frames per condition drawn from different cameras and each carrying that condition alone: (A) Clear, (B) Glare, (C) Fog, (D) Rain/Blur, (E) Hazy, (F) Dark. Clear frames show a resolved horizon and surf zone; Glare frames show saturation on the water surface; Fog frames lose the horizon and distant surf; Rain/Blur frames show lens droplets, streaking or defocus; Hazy frames show reduced contrast with the horizon still discernible; Dark frames are pre-dawn, deep-overcast or post-dusk scenes that remain interpretable. The figure shows the range of scene appearance each label covers across cameras and sites.

2.2 Classifier

The classifier is the smallest (nano) YOLO26 classification network of the Ultralytics framework (Ultralytics, 2025), 1.6 million parameters with a 91-class output head, initialised from the publisher's ImageNet weights and fine-tuned on the label-powerset classes. The whole frame is resized anisotropically to a 224×224 square; pixel values are scaled to the unit interval with no further normalisation. Augmentation is restricted to horizontal flips: brightness, saturation, contrast and random-erasing augmentations are disabled. Training runs for at most 60 epochs with the framework's default optimiser and schedule and stops after 15 epochs without improvement on a validation split. The output is a probability over the 91 strings; the predicted string is the most probable one, and its first condition is the primary label.

2.3 Evaluation

Three protocols are used, differing only in how the labelled frames are partitioned. Each answers one of the questions the paper addresses, and all three score the

Figure 3: Canonical multi-rank labelling examples reproduced from the annotators' written guide. Each panel's title gives the rank order, primary condition first: (A) Clear, Glare; (B) Clear, Hazy; (C) Clear, Rain/Blur; (D) Clear, Fog; (E) Glare, Clear; (F) Glare, Hazy; (G) Hazy, Clear; (H) Hazy, Rain/Blur; (I) Hazy, Dark; (J) Fog, Clear; (K) Rain/Blur, Clear; (L) Rain/Blur, Dark; (M) Dark, Clear; (N) Dark, Hazy; (O) Glare, Dark, Hazy; (P) Hazy, Clear, Glare. The reversed pairs (A)/(E), (B)/(G), (C)/(K), (D)/(J) and (I)/(N) show the surf-zone-area convention: the same pair of conditions receives opposite rank orderings depending on which condition affects more of the surf zone. Panels (O) and (P) are the rare cases in which a third rank is required.

same predicted label strings with the same metrics.

2.3.1 Test Split

The 33,569 frames are divided at random into a training set (24,170 frames), a validation set (2,686 frames, roughly one tenth of the training frames, stratified by primary label) on which the training epoch is selected, and a test set (6,713 frames, 20% of all frames) that is scored once with the selected network. The split is at the frame level, so cameras that appear in training also appear in the test set.

2.3.2 Cameras Absent From Training

To measure accuracy on a camera the classifier has never seen, all 33,569 frames are pooled and scored out-of-fold under a five-fold protocol in which every frame of a camera falls in the same fold (a grouped partition on the resolved camera identity; Roberts *et al.*, 2017). Each fold's network is trained for a fixed 35 epochs with no validation split. The pooled out-of-fold predictions are scored as the test split is, and additionally by the number of labelled frames each camera contributes.

2.3.3 Labelled Examples per Camera

To measure what a labelled example of a condition on a camera contributes, one condition at a time is withheld from a set of cameras. For each degraded condition, half of the cameras with at least three training frames of that condition, selected at random, are held out: their training frames whose primary label is that condition are removed, their other frames are kept. Recall of the withheld condition is then measured on the test frames of that condition from the held-out cameras (a camera the classifier has seen, but never in this condition) and compared with the recall of the full classifier on the same frames, with recall on the same condition from the retained cameras, and with recall on cameras absent from training. Bootstrap intervals (2,000 resamples over frames) accompany each recall.

3 Results

Results are reported on the 6,713-frame test split, under the camera-disjoint folds over all 33,569 frames, and under the condition holdout. Accuracy is given for the ordered label string and for the primary label alone, with per-class precision, recall and F1 on primary labels. The three protocols are reported in turn, and each is scored with the same metrics so that the regimes can be compared directly.

3.1 Test Split

Table 1 reports accuracy on the test split. Primary-label accuracy is 93.1% and exact multi-rank accuracy 84.1%, against 67.9% for always predicting the majority class; the 9.0-point difference between the two accuracies is the rate at which the primary condition is right but a secondary condition is omitted, added or reordered. Validation and test figures agree to within one point.

Table 1: Accuracy of the classifier on the validation split used to select the training epoch and on the 6,713-frame test split, scored once. Primary-label accuracy compares the first-listed predicted condition with the first-listed ground-truth condition; exact multi-rank accuracy requires the whole ordered label string to match; macro-F1 averages the per-class F1 of the six primary conditions; the majority-class rate is the accuracy of always predicting Clear. The validation column is the split on which the training epoch was chosen and is therefore not a second held-out estimate; the test column is the held-out estimate of accuracy. The table shows the margin over the majority class, the cost of requiring the full multi-rank string, and that the two columns agree to within one point on every metric, so selecting the epoch on the validation split did not inflate the reported accuracy.

Metric	Validation	Test
Primary-label accuracy (%)	93.3	93.1
Exact multi-rank accuracy (%)	85.0	84.1
Macro-F1 over primary labels	0.884	0.878
Majority-class rate (%)	67.9	67.9
Frames	2,686	6,713

Table 2 reports per-class precision, recall and F1 on primary labels. F1 ranges from 0.96 for Clear to 0.79 for Hazy, whose recall of 0.75 is the lowest of any class; the four other degraded conditions have recall between 0.86 and 0.89.

Figure 4 shows the confusion matrix on primary-label predictions normalised by true class. The largest off-diagonal entries are in the Clear column: 16% of Hazy frames are predicted as Clear, 11% of Glare, 8% of Rain/Blur, 7% of Dark and 7% of Fog. Confusion between pairs of degraded conditions does not exceed 5% (Hazy predicted as Rain/Blur).

Table 2: Per-class precision, recall and F1 on primary-label predictions on the test split. N is the number of test frames with that primary label. The table shows where the error concentrates: Hazy has the lowest recall and F1, and the other four degraded conditions are recalled at 0.86 to 0.89.

Class	Precision	Recall	F1	N
Clear	0.95	0.97	0.96	4,561
Glare	0.90	0.87	0.89	688
Fog	0.90	0.89	0.89	302
Rain/Blur	0.90	0.86	0.88	595
Hazy	0.84	0.75	0.79	382
Dark	0.84	0.89	0.86	185

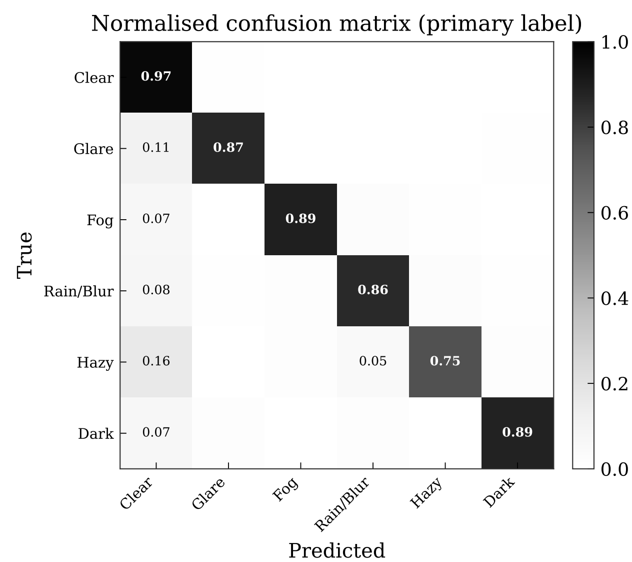

Figure 4: Row-normalised confusion matrix for primary-label predictions on the test split. Rows are true conditions, columns predicted conditions, and each cell gives the fraction of the row's frames that received that prediction, so the diagonal is per-class recall; off-diagonal cells below 0.03 are left blank. The figure shows that the dominant off-diagonal mass lies in the Clear column, largest for Hazy (16%) and Glare (11%), and that confusion between pairs of degraded conditions is small by comparison.

3.2 Cameras Absent From Training

Table 3 reports the camera-disjoint folds, in which every camera is scored by a network that has not seen it. Pooled over all 33,569 frames, primary-label accuracy is 81.0% (fold range 76.5 to 84.3%), exact multi-rank accuracy 61.1% and macro-F1 0.62, against a majority-class rate of 67.9%. Clear is recalled at 0.90, Glare and Rain/Blur at 0.75, and Fog, Dark and Hazy at 0.43, 0.43 and 0.38; between 20% and 45% of the frames in each of Glare, Fog, Hazy and Dark are predicted as Clear, and 22% of Hazy frames as Rain/Blur.

Table 4 splits both regimes by the number of labelled frames a camera contributes. For the 483 cameras with 6 to 20 labelled frames, accuracy is 82.7% in both regimes. For the 241 cameras with more than 20 frames, which hold 83% of the dataset, the test split scores 95.3% and the camera-disjoint folds 80.7%. The table omits the seven cameras with a single labelled frame.

3.3 Labelled Examples per Camera

Table 5 gives the design of the condition holdout, and Table 6 and Figure 5 report recall of each degraded condition by what the camera contributed in training. On cameras that contributed labelled examples of the condition, recall is 91 to 97%. On cameras whose examples of the condition were withheld, recall falls to 77% for Rain/Blur, 64% for Fog, 45% for Glare, 19% for Dark and 16% for Hazy. The full classifier recalls 86 to 99% of the same frames. For Glare, Hazy and Dark, recall on a camera seen without the condition (45, 16 and 19%) is below recall on a camera absent from training altogether (75, 38 and 43%, from the camera-disjoint folds).

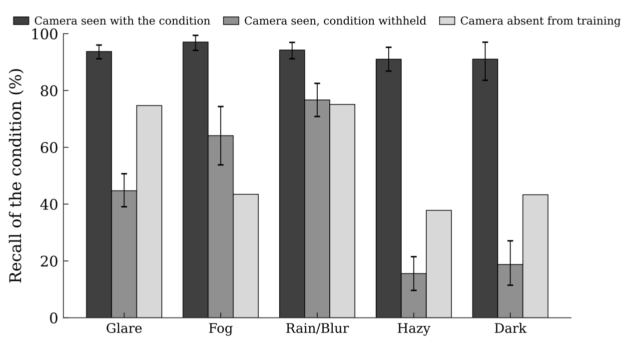

Figure 5: Recall of each degraded condition under three training regimes: the camera contributed labelled examples of the condition (dark bars), the camera is in training but its examples of the condition were withheld (mid-grey bars), and the camera is absent from training altogether (light bars, camera-disjoint folds). Error bars are 95% bootstrap intervals over test frames (none for the pooled fold estimate). The figure shows how much of each condition's recall depends on the camera's own examples: little for Rain/Blur, most for Hazy and Dark.

4 Discussion

The classifier's errors concentrate on the boundary between mildly degraded frames and Clear; its accuracy on a camera depends on how that camera is represented in training, and for three of the five degraded conditions on whether that camera was labelled in that condition at all. The error structure is considered first, then the difference between the two cross-validation regimes, then what a labelled example of a condition on a camera contributes. The limitations of the evaluation close the section.

4.1 Error Structure

On the test split the largest off-diagonal entries of the confusion matrix are in the Clear column: 16% of Hazy frames, 11% of Glare frames and 7 to 8% of Fog, Rain/Blur and Dark frames are predicted as Clear, whereas confusion between pairs of degraded conditions does not exceed 5%. Clear holds 68% of the frames, and a mildly degraded frame whose appearance overlaps a typical clear frame of the same camera is resolved toward the majority. Hazy is the weakest condition (F1 = 0.79, recall = 0.75): a frame labelled Hazy might represent intermediate atmospheric attenuation on a continuum between Clear and Fog, and some fraction of borderline frames is ambiguous to a single-frame classifier and to a human annotator.

The same conservative bias, higher precision than recall on the degraded classes with marginal frames read as Clear, is reported by Rauschenbach *et al.* (2026) for a Gaussian-process fog classifier on handcrafted statistics, evaluated on a subset of the same camera network; their fog F1 of 0.87 is comparable to the Fog F1 of 0.89 here, on a two-class task with a different reference.

4.2 Cameras Absent From Training

The test split and the camera-disjoint folds estimate different quantities (Roberts *et al.*, 2017). The test split estimates accuracy on new frames from cameras already in training, which is the regime in which the classifier operates; the folds estimate accuracy on a camera with no labelled history. The difference, 93.1% against 81.0% primary-label accuracy, is carried by the conditions rather than by Clear: Clear is recalled at 0.90 on unseen cameras, Glare and Rain/Blur at 0.75, and Fog, Dark and Hazy at 0.38 to 0.43, with a fifth to almost half of their frames read as Clear. Table 4 locates the difference in the cameras with many labelled frames: on the 483 cameras with 6 to 20 labelled frames the two regimes agree at 82.7%, whereas on the 241 cameras with more than 20 frames the test split scores 95.3% and the folds 80.7%. The test-split accuracy is therefore set by cameras with a large labelled history, on which the network has learned camera-specific appear-

Table 3: Accuracy on cameras the classifier has seen against cameras it has not. The first row is the test split of Table 1; the second is the five-fold camera-disjoint cross-validation over all 33,569 frames, in which every frame of a camera falls in the same fold and each fold's network is trained for a fixed 35 epochs. Columns give primary-label and exact multi-rank accuracy (%), macro-F1 over primary labels, and per-class recall. The table separates accuracy within the labelled camera set from accuracy on a camera with no labelled history, and shows that the loss falls on Fog, Hazy and Dark.

Cameras	Primary	Exact	Macro-F1	Clear	Glare	Fog	Rain/Blur	Hazy	Dark
In training (test split)	93.1	84.1	0.878	0.97	0.87	0.89	0.86	0.75	0.89
Unseen (folds)	81.0	61.1	0.616	0.90	0.75	0.43	0.75	0.38	0.43

Table 4: Primary-label accuracy on the test split and under the camera-disjoint folds for cameras grouped by their number of labelled frames, with the number of cameras and labelled frames in each group. The table shows that the two regimes agree for cameras with 20 or fewer labelled frames and diverge for the 241 cameras with more, which supply most of the frames.

Frames per camera	Cameras	Frames	Test split	Cameras unseen
2–5	26	103	73.9%	70.9%
6–20	483	5,684	82.7%	82.7%
21 or more	241	27,775	95.3%	80.7%

Table 5: Design of the condition holdout. For each degraded condition, the cameras with at least three training frames of it were eligible; a random half of them were held out and every training frame of theirs with that primary label was removed before retraining. The last column is the number of test frames of the condition from the held-out cameras on which the withheld-condition recall of Table 6 is measured. The table gives the sample sizes behind that table.

Condition	Eligible cameras	Held out	Frames removed	Held-out test frames
Glare	148	74	1,101	284
Fog	30	15	260	78
Rain/Blur	140	70	913	223
Hazy	85	42	543	135
Dark	63	31	326	96

ance, and a camera with few labels scores about 83% whether or not it is in training.

4.3 Labelled Examples per Camera

A camera's labelled frames contribute its appearance in general and its appearance in each labelled condition, and the condition holdout separates the two. Rain/Blur is recognised without the second: a camera never labelled for it keeps 77% recall, and a camera absent from training 75%. Fog and Glare are recognised partly (64% and 45%). Hazy and Dark are recognised almost only where the camera's own examples exist: 16% and 19% without them, against 90 to 92% for the full classifier on the same frames.

For Glare, Hazy and Dark, a camera that is in training without the condition does worse than a camera

Table 6: Recall of each degraded condition (%, with 95% bootstrap interval over test frames) by what the camera contributed in training. With condition: the full classifier on test frames of the condition from cameras whose examples of it were kept. Without condition: the classifier retrained without the held-out cameras' examples of the condition, on those cameras' test frames of it. Full, same frames: the full classifier on those same held-out frames. Camera unseen: recall under the camera-disjoint folds of Table 3. The table shows that Rain/Blur transfers to a camera without its own example, Fog and Glare partly, and Hazy and Dark hardly at all.

Condition	With condition	Without condition	Full, same frames	Camera unseen
Glare	94 [91, 96]	45 [39, 51]	86 [82, 90]	75
Fog	97 [94, 99]	64 [54, 74]	99 [96, 100]	43
Rain/Blur	94 [91, 97]	77 [71, 83]	94 [90, 97]	75
Hazy	91 [87, 95]	16 [10, 22]	90 [85, 96]	38
Dark	91 [84, 97]	19 [11, 27]	92 [86, 97]	43

that is not in training at all (45 against 75%, 16 against 38%, 19 against 43%). The network learns each camera's usual appearance from its labelled frames, and a condition it has never seen on that camera is resolved toward the camera's usual label. In operation a camera enters the training set when frames from it are labelled. If those frames show clear conditions only, recall of haze, low light and glare on that camera falls below what it was before the camera was labelled. Labels for a new camera therefore have to include its first hazy, dark and glare-affected segments; Rain/Blur is recognised without a per-camera example.

4.4 Limitations

The six conditions are usability judgements for the downstream segmentation and detection modules and have no external physical reference. The boundary between Hazy and light Fog, and between Dark and heavily overcast Clear, is a judgement rather than a measurement; no inter-annotator agreement study was conducted, and the written protocol is the mechanism by which one standard is held across annotators and over time. The label ceiling in the transitional classes is therefore unmeasured, and any systematic bias shared by the annotators is inherited by the classifier and invisible to the evaluation. Because the condition holdout withholds a condition only where it is the primary label, the held-out cameras were not entirely free of it in training, and the effect reported in Table 6 is a lower bound on what withholding every example would produce.

Seasonal and diurnal coverage follows the labelling campaigns rather than a sampling design. Each frame is classified independently, although visibility transitions are smooth and temporally correlated: the classifier scores the first frame of each 10-minute segment, the label is applied to the whole segment, and no rolling window over consecutive predictions is used. This holds for slowly varying conditions such as fog, haze and darkness, and less so for transient or onsetting conditions such as glare, which can develop within one segment.

5 Conclusions

A compact convolutional classifier tags six co-occurring visibility conditions on frames from a 757-camera coastal network at 93.1% primary-label and 84.1% exact multi-rank accuracy, with per-class F1 from 0.96 for Clear to 0.79 for Hazy, on a 6,713-frame test split drawn from cameras it was trained on.

On a camera it has never seen, primary-label accuracy is 81.0% against a majority-class rate of 67.9%; Clear, Glare and Rain/Blur are recognised there, and Fog, Hazy and Dark are recognised in fewer than half of their frames.

Whether a camera has been labelled in a condition decides whether the condition is recognised on it. Rain/Blur transfers to a camera without its own example, Fog and Glare in part, Hazy and Dark hardly at all, and a camera labelled only in other conditions is worse for glare, haze and low light than a camera never labelled. Labels gathered when a new camera joins the network therefore have to include its hazy and dark segments; clear-weather frames alone lower its recall of those conditions on that camera.

Acknowledgements

This is version 2 of this preprint (EarthArXiv, doi:10.31223/X5FN5W). Version 1, posted 30 July 2026, reported an earlier visibility classifier for the same task, evaluated on a subset of the frames used here; it shares no results with this version and is superseded by it. This version was submitted to the *Journal of Coastal Research* as a Technical Communication on 7 September 2026 and is under review. The companion paper describing the object detector that runs downstream of the visibility classifier (Reinwald *et al.*, 2026, cited in the Introduction) has been submitted separately to the *Journal of Coastal Research*; it concerns a different model and shares no results with this paper.

B. Freeston, a co-author of this paper, is the named inventor on US Patent 10,891,481 B2 (Freeston, 2021), assigned to Surfline/Wavetrak, Inc., which discloses the broader automated ocean-sensing framework within which the classifier was developed.

All authors are employees of Surfline/Wavetrak, Inc., which operates the camera network and the classifier described in this paper, and which funded the work. No external funding was received. Frames were labelled on the Encord annotation platform.

The labelled frames and the trained network weights are proprietary to Surfline/Wavetrak, Inc., and are not released. The network architecture and its published pretrained weights are public (Ultralytics, 2025); the label scheme, the labelling protocol as summarised in the Annotation Methodology subsection, the training configuration, the evaluation protocols and every reported figure are given in full in this paper.

Literature Cited

Bae, T.W.; Han, J.H.; Kim, K.J., and Kim, Y.T., 2019. Coastal visibility distance estimation using dark channel prior and distance map under sea-fog: Korean Peninsula case. *Sensors*, 19(20), 4432.

Boutell, M.R.; Luo, J.; Shen, X., and Brown, C.M., 2004. Learning multi-label scene classification. *Pattern Recognition*, 37(9), 1757–1771.

Bronte, S.; Bergasa, L.M., and Alcantarilla, P.F., 2009. Fog detection system based on computer vision techniques. *In: Proceedings of the 12th International IEEE Conference on Intelligent Transportation Systems* (St. Louis, Missouri), pp. 1–6.

Choi, L.K.; You, J., and Bovik, A.C., 2015. Referenceless prediction of perceptual fog density and perceptual image defogging. *IEEE Transactions on Image Processing*, 24(11), 3888–3901.

Freeston, B., 2021. *Automated Detection of Features and/or Parameters within an Ocean Environment Using Image Data.* Alexandria, Virginia: United States Patent and Trademark Office, U.S. Patent No. 10,891,481 B2, assigned to Surfline/Wavetrak, Inc.

Harley, M.D.; Kinsela, M.A.; Sánchez-García, E., and Vos, K., 2019. Shoreline change mapping using crowd-sourced smartphone images. *Coastal Engineering*, 150, 175–189.

Hautière, N.; Tarel, J.-P.; Lavenant, J., and Aubert, D., 2006. Automatic fog detection and estimation of visibility distance through use of an onboard camera. *Machine Vision and Applications*, 17(1), 8–20.

Holman, R.A. and Stanley, J., 2007. The history and technical capabilities of Argus. *Coastal Engineering*, 54(6–7), 477–491.

Lewis, J.M.; Koračin, D.; Rabin, R., and Businger, J., 2003. Sea fog off the California coast: viewed in the context of transient weather systems. *Journal of Geophysical Research: Atmospheres*, 108(D15), doi:10.1029/2002JD002833.

Lu, C.; Lin, D.; Jia, J., and Tang, C.-K., 2014. Two-class weather classification. *In: Proceedings of the IEEE Conference on Computer Vision and Pattern Recognition* (Columbus, Ohio), pp. 3718–3725.

Mittal, A.; Moorthy, A.K., and Bovik, A.C., 2012. No-reference image quality assessment in the spatial domain. *IEEE Transactions on Image Processing*, 21(12), 4695–4708.

Rauschenbach, S.; Kim, J.B.; Dye, A.W.; Faloona, I.; Rockwood, R.C.; Still, C.J.; Paw U, K.T., and Igel, A.L., 2026. A characterization of local spatio-temporal variability in daytime occurrence of fog along the Oregon coast using public cameras and airport weather metrics. *Agricultural and Forest Meteorology*, 388, 111315.

Reinwald, M.; Mitchell-Wynne, K.; D'Amico, Z.; Stringer, M., and Freeston, B., 2026. SCI-OBS: Detection and classification of people on the beach and in the surf zone. *EarthArXiv*, non-peer-reviewed preprint, doi:10.31223/X5VV3X.

Roberts, D.R.; Bahn, V.; Ciuti, S.; Boyce, M.S.; Elith, J.; Guillera-Arroita, G.; Hauenstein, S.; Lahoz-Monfort, J.J.; Schröder, B.; Thuiller, W.; Warton, D.I.; Wintle, B.A.; Hartig, F., and Dormann, C.F., 2017. Cross-validation strategies for data with temporal, spatial, hierarchical, or phylogenetic structure. *Ecography*, 40(8), 913–929.

Splinter, K.D.; Harley, M.D., and Turner, I.L., 2018. Remote sensing is changing our view of the coast: insights from 40 years of monitoring at Narrabeen-Collaroy, Australia. *Remote Sensing*, 10(11), 1744.

Tsoumakas, G. and Katakis, I., 2007. Multi-label classification. *International Journal of Data Warehousing and Mining*, 3(3), 1–13.

Ultralytics, 2025. *Ultralytics YOLO*. `https://github.com/ultralytics/ultralytics`.

Yang, W.; Zhao, Y.; Li, Q.; Zhu, F., and Su, Y., 2023. Multi visual feature fusion based fog visibility estimation for expressway surveillance using deep learning network. *Expert Systems with Applications*, 234, 121151.